Cascade Fuzzy Neural Network Control for Ball and Beam Systems

Hung-Wei Lin[1,*], Wei-Shou Chan[2], and Chun-Yi Lee[2]

[1]*Department of Electrical Engineering, Lee-Ming Institute of Technology*
[2]*Department of Electrical Engineering, Chang Gung University*

ABSTRACT

In this paper, a ball and beam experiment platform is considered. Based on a fuzzy neural network (FNN), a desired positioning controller can be obtained subject to extraneous disturbances. A FNN structure not only preserves the fuzzy linguistic description logic, but also has the parameter-learning capability of neural networks. In this paper, a cascaded inner-outer loop scheme is constructed for the ball and beam system, where the controller parameters of the inner loop FNN can be adaptively tuned using gradient decent method. Simulation and experimental results indicate that the proposed cascade FNN control scheme can provide better robust responses.

Keywords: fuzzy neural network, ball-and-beam system, gradient decent method.

球與桿系統之串接式模糊類神經控制

林淯偉[1*] 詹為守[2] 李俊毅[2]

[1]黎明技術學院電機系
[2]長庚大學電機系

摘 要

本論文針對一個球與桿實驗平台，在存有外部干擾的情況下，採用模糊類神經網路控制架構，完成一個所需的定位控制器設計。模糊類神經網路可保留傳統模糊邏輯的語意表達，另兼具類神經系統的參數學習能力。在本文中，球與桿系統建構在一個串接式的內外迴路架構；其中，外迴路的模糊類神網路控制器參數可透過最陡坡降法完成線上學習。經由模擬與實驗結果得知，本文所提出的串接式模糊類神經網路控制架構具有較佳的強健性能響應。

關鍵詞：模糊類神經網路、球與桿系統、梯度坡降法

文稿收件日期 102.2.26;文稿修正後接受日期 103.1.17; *通訊作者
Manuscript received February 26, 2013; revised January 17, 2014; * Corresponding author

Ⅰ. INTRODUCTION

The study of under-actuated nonlinear systems has attracted considerable attention over the past years. [1-5].Under-actuated systems can be found in real life; examples of such systems include ball-and-beam system, pendulum-cart system. An under-actuated system has fewer control inputs than degrees of freedom that cause the challenges for tracking control.

Ball and beam system is a popular benchmark platform in academics because of the inherent nonlinearity and instability. In [6], the set-point balance control problem was addressed for a ball and beam system, where the total mechanical energy and passivity properties were considered. Many control schemes have been proposed for ball-and-beam systems, such as PD cascade controller and fuzzy cascade controller [7]. The fuzzy cascade controller consists of two control loops, where the inner- and outer-loop controllers are discussed for the control of beam angle and ball position, respectively. PID controllers have been used extensively in the industries due to their simplicity for operation. However, with the increasing complexity of control systems, a typical PID controller usually fails to meet high-performance requirements subject to uncertainties. In the last 30 years, fuzzy control techniques have been widely addressed in many applications [10, 11]. Fuzzy logic control consisting of linguistic control rules is a technique to design controllers based on expert knowledge and experience. Unlike model-based techniques, fuzzy logic approaches can be performed well without knowing exact system model even with unexpected complex dynamics and external disturbances [12, 13]. Therefore, fuzzy logic control (FLC) has been successfully implemented in many practical applications and has also been shown in some cases to outperform traditional control systems [14, 15].

Recently, fuzzy neural networks (FNN), combining the capability of fuzzy reasoning to handle uncertain information and the capability of artificial neural networks to learn from processes, have been popularly addressed. In [16], an adaptive fuzzy neural network control system was proposed to control the mover position of a field-oriented control permanent magnet linear synchronous motor. In [17], a robust FNN control scheme including a parameter tuning algorithm was designed for the levitated positioning of a linear Maglev rail system. A neural network based self-learning control strategy consisting of a FNN controller and a recurrent neural network identifier was proposed for electronic throttle valves [18]. In [19], an adaptive network-based fuzzy inference system was presented for speed and position estimation of a permanent-magnet synchronous generator. However, the FNN control of an under-actuated system has not been addressed in the above papers.

In this paper, a cascaded inner-outer loop configuration is presented for a ball and beam system, in which noise and disturbance are considered. The proposed controller combines the FLC and a neural network, where the update laws of network parameters are obtained based on the gradient decent method. In addition to simulations, a DSP/FPGA based ball-and-beam experimental system is applied to validate the feasibility of the proposed works.

The organization of this paper is as follows. In Sec. II, the dynamic characteristics of the ball and beam system are discussed. The design procedures of a cascade FNN will be introduced in Sec. III. Parameter-learning algorithm is addressed in Sec. IV. In Sec. V, simulation and experimental results are provided for performance validations. The concluding remarks are given in Sec. VI.

Ⅱ. BALL AND BEAM SYSTEM

The configuration of an end-point driven ball and beam system is shown in Fig.1, where o0 is the small gear mounted on a DC motor, o1 represents the big gear that can control the beam angle, and o2 is the pivot. The system parameters for the ball and beam system model are listed in Table 1.

Let the state vector of the ball and beam system be defined as $x(t) = [x1(t)\ x2(t)\ x3(t)\ x4(t)]T$, where x1(t) is the ball position (m), x2(t) is the ball velocity (m/sec), x3(t) is the beam angle (rad), and x4(t) is the angular velocity of the beam (rad/sec). The mathematical model of the ball and beam system can be represented as follows [20, 21]:

$$\dot{x}_1 = x_2$$
$$\dot{x}_2 = Ax_1x_4^2 - Ag\sin x_3$$
$$\dot{x}_3 = x_4$$
$$\dot{x}_4 = B(x_1)\cos x_3[C\cos(lx_3d^{-1})u - Dx_4\cos(lx_3d^{-1}) - E - Fx_1] - B(x_1)Gx_1x_2x_4, \quad (1)$$

where $A = (1+m_B^{-1}J_BR^{-2})^{-1}$, $B(x_1)=(J_B+J_b+m_Bx_1^2)^{-1}$, $C=nK_bl(R_ad)^{-1}$, $D=(nK_bl)^2(R_ad^2)^{-1}$, $E=0.5lm_bg$, $F=m_Bg$, $G=2m_B$, and u is the input voltage of the DC motor.

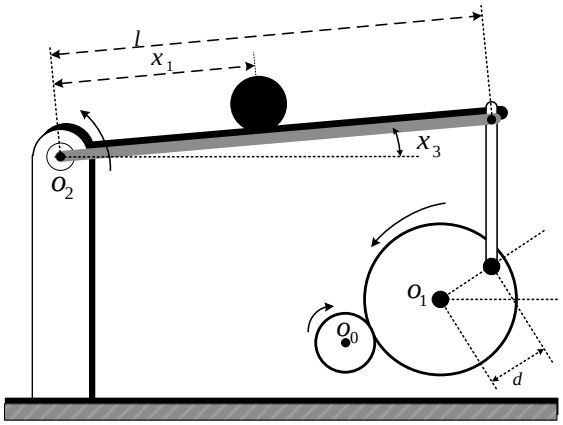

Fig. 1. Scheme diagram of the ball and beam system.

TABLE 1. Parameters of the ball and beam system.

Symbol	Definition	Value
m_B	mass of the ball	0.029kg
m_b	mass of the beam	0.334kg

Table 1. PARAMETERS OF THE BALL AND BEAM SYSTEM (CONTINUE)

Symbol	Definition	Value
R	radius of the ball	0.0095m
l	beam length	0.4m
d	radius of the large gear	0.04m
J_B	ball inertia	$1.05\text{x}10^{-6}$ kgm^2
J_b	beam inertia	0.0178kgm^2
K_b	back-EMF constant	0.1491Nm/A
R_a	armature resistance	18.91Ω
g	acceleration of gravity	9.8m/s^2
n	gear ratio	4.2

Ⅲ. CASCADE FNN CONTROLLER DESIGN

The proposed cascade FNN control scheme of a ball and beam system is shown in Fig. 2, where each controller has two inputs. For example, the position error and the derivative of position error are the input variables of the outer-loop fuzzy controller. In Fig. 2, FNN and FLC are used for the inner- and outer-loop control, respectively. In addition, ISF1, ISF2, ISF3 and ISF4 are input scale factors, and OSF1 and OSF2 are output scale factors. The objective of the controller design is to make the ball position x1 follow the reference command x1d. The position error of ball tracking is defined as e1 = x1d - x1. In this paper, the goal is to stabilize the ball to a desired position x1d = 0.2m.

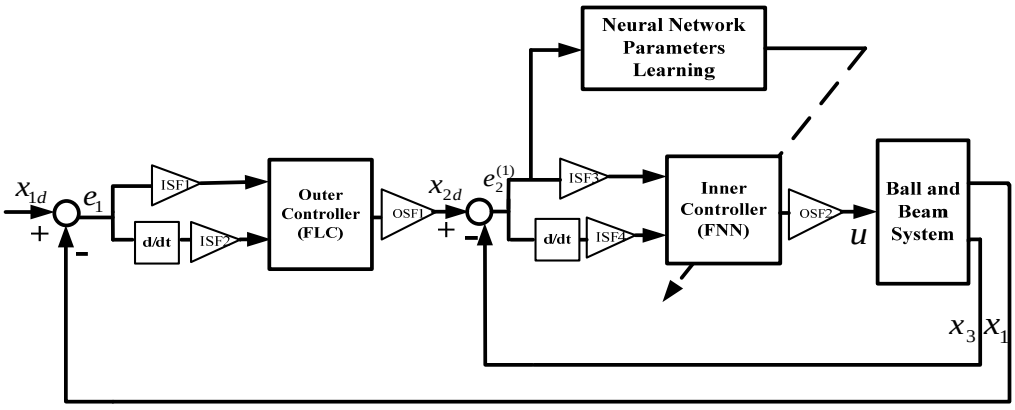

Fig. 2. The cascaded control structure of the ball and beam system.

In general, a FLC controller consists of linguistic "IF-THEN" rules that can be constructed using the knowledge of experts in the given field of interest. The If-Then rules can be expressed as

$$R_j: \text{If } e_1 \text{ is } \tilde{F}_{1j} \text{ and } \dot{e}_1 \text{ is } \tilde{F}_{2j}, \text{ then } x_{2d} \text{ is } w_j, \quad (2)$$

where e_1 and $\dot{e}_1$ are the inputs of FLC, $\tilde{F}_{1j}$ and $\tilde{F}_{2j}$ are antecedent membership functions, and G_j is the consequent membership function, j=1, 2, ..., m.

The structure of FNN is shown in Fig. 3. The "IF-THEN" rules for FNN can be expressed as

$$R_j: \text{If } e_2^{(1)} \text{ is } \tilde{F}_{1j}^{(2)} \text{ and } \dot{e}_2^{(1)} \text{ is } \tilde{F}_{2j}^{(2)}, \text{ then } u \text{ is } w_j^{(4)}, \quad (3)$$

where $e_2^{(1)}$ and $\dot{e}_2^{(1)}$ are the inputs of FNN, $\tilde{F}_{1j}^{(2)}$ and $\tilde{F}_{2j}^{(2)}$ are antecedent membership functions, $G_j^{(4)}$ is the consequent membership function, j=1, 2, ..., m. The function of each layer of the FNN will be introduced in the following.

1) Input layer:

From Fig. 2, x2d is the output of the outer controller. Let e2(1) = x2d - x3 be the tracking error of the beam angle. The change of e2(1) is denoted as $\dot{e}_2^{(1)}$.

2) Membership layer:

In this layer, each node performs as a Gaussian membership function. For example, the function of the jth node is represented as

$$\mu_{\tilde{F}_{1j}}^{(2)}(e_2^{(1)}) = \exp\left\{-\frac{1}{2}\left(\frac{e_2^{(1)} - m_{1j}^{(2)}}{\sigma_{1j}^{(2)}}\right)^2\right\}, \quad (4)$$

$$\mu_{\tilde{F}_{2j}}^{(2)}(\dot{e}_2^{(1)}) = \exp\left\{-\frac{1}{2}\left(\frac{\dot{e}_2^{(1)} - m_{2j}^{(2)}}{\sigma_{2j}^{(2)}}\right)^2\right\}, \quad (5)$$

where $m_{1j}^{(2)}$ ($m_{2j}^{(2)}$) and $\sigma_{1j}^{(2)}$ ($\sigma_{2j}^{(2)}$) are means and standard deviations, respectively, j = 1, 2, ..., n.

3) Rule layer:

The rule layer is performed to multiply its input signals and output the result of product. The product output of the jth node is determined as

$$f_j^{(3)} = \prod_{i=1}^{2} \mu_{\tilde{F}_{ij}}^{(2)}. \quad (6)$$

4) Output layer:

The output layer is performed as a de-fuzzy process. Considering the singleton consequent membership functions, the output of this layer can obtained as

$$y^{(4)} = \frac{\sum_{j=1}^{n} f_j^{(3)} w_j^{(4)}}{\sum_{j=1}^{n} f_j^{(3)}} = u(t). \quad (7)$$

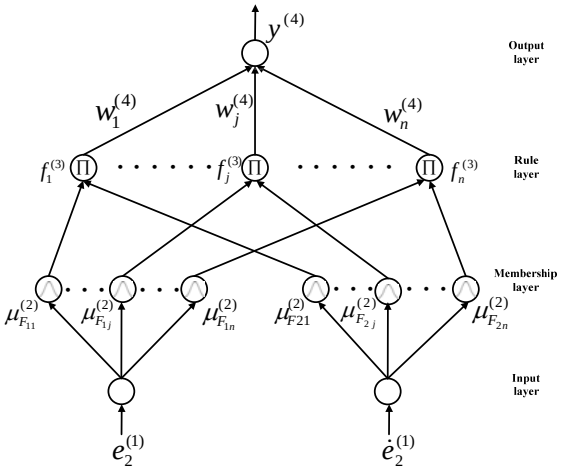

Fig. 3. The structure of FNN.

Ⅳ. PARAMETER-LEARNING ALGORITHM

The procedures to derive an online learning based on the supervised gradient descent method will be illustrated in this section. First, the cost function is defined as

$$E = \frac{1}{2}(x_{2d} - x_3)^2 = \frac{1}{2}(e_2^{(1)})^2. \quad (8)$$

Then, the update laws of the FNN parameters are described as follows. The means and standard deviations of the antecedent membership functions are updated as follows

$$m_{ij}^{(2)}(k+1) = m_{ij}^{(2)}(k) - \eta_m \frac{\partial E}{\partial m_{ij}^{(2)}}, \quad (9)$$

$$\sigma_{ij}^{(2)}(k+1)=\sigma_{ij}^{(2)}(k)-\eta_{\sigma}\frac{\partial E}{\partial \sigma_{ij}^{(2)}}, \tag{10}$$

where i=1,2, j=1,2,...,n., $k=1,2,3,...,N$ denotes the iteration number, and η_m and η_σ are learning -rates parameters of the means and standard deviation, respectively. The consequent membership functions are updated according to the following adaptive rules

$$w_j^{(4)}(k+1)=w_j^{(4)}(k)-\eta_w\frac{\partial E}{\partial w_j^{(4)}} \tag{11}$$

where i = 1, 2, j = 1, 2, ..., n., $k=1,2,3,...,N$, and η_w is a learning-rate parameters of the consequent membership function. In (9)-(11), the detail calculations of $-\frac{\partial E}{\partial m_{ij}^{(2)}}$, $-\frac{\partial E}{\partial \sigma_{ij}^{(2)}}$ and $-\frac{\partial E}{\partial w_j^{(4)}}$ can be determined as follows.

1) Output layer:

The error term to be propagated is computed as

$$\delta^{(4)}=\frac{-\partial E}{\partial y^{(4)}}=\frac{\partial E}{\partial x_3}\frac{\partial x_3}{\partial y^{(4)}}. \tag{12}$$

It is noticed that $\frac{\partial x_3}{\partial y^{(4)}}$ cannot be analytically determined. To overcome this problem, the adaptive law proposed in [22] is adopted as follows

$$\delta^{(4)}=e_2^{(1)}=(x_{2d}-x_3). \tag{13}$$

It can be obtained that

$$\frac{-\partial E}{\partial w_j^{(4)}}=\delta^{(4)}\frac{\partial y^{(4)}}{\partial w_j^{(4)}}, \tag{14}$$

$$\frac{\partial y^{(4)}}{\partial w_j^{(4)}}=\frac{f_j^{(3)}w_j^{(4)}}{\sum_{j=1}^{n}f_j^{(3)}}. \tag{15}$$

where j = 1, 2, ..., n.

2) Rule layer:

The error term is calculated as follows

$$\begin{aligned}\delta_j^{(3)}&=\frac{-\partial E}{\partial f_j^{(3)}}=\frac{-\partial E}{\partial y^{(4)}}\frac{\partial y^{(4)}}{\partial f_j^{(3)}}\\&=\delta^{(4)}\cdot\frac{w_j^{(4)}\cdot\sum_{j=1}^{n}f_j^{(3)}-\sum_{j=1}^{n}f_j^{(3)}w_j^{(4)}}{(\sum_{j=1}^{n}f_j^{(3)})^2}\\&=\delta^{(4)}\cdot\frac{(w_j^{(4)}-y^{(4)})}{\sum_{j=1}^{n}f_j^{(3)}},\end{aligned} \tag{16}$$

in which j = 1, 2, ..., n.

3) Membership layer:

The error term is computed as follows

$$\delta_{1j}^{(2)}=\frac{-\partial E}{\partial \mu_{\tilde{F}_{1j}}^{(2)}(e_2^{(1)})}=\delta_j^{(3)}\cdot\frac{\partial f_j^{(3)}}{\partial \mu_{\tilde{F}_{1j}}^{(2)}(e_2^{(1)})}=\delta_j^{(3)}\cdot\mu_{\tilde{F}_{2j}}^{(2)}(\dot{e}_2^{(1)}), \tag{17}$$

$$\delta_{2j}^{(2)}=\frac{-\partial E}{\partial \mu_{\tilde{F}_{2j}}^{(2)}(\dot{e}_2^{(1)})}=\delta_j^{(3)}\cdot\frac{\partial f_j^{(3)}}{\partial \mu_{\tilde{F}_{2j}}^{(2)}(\dot{e}_2^{(1)})}=\delta_j^{(3)}\cdot\mu_{\tilde{F}_{1j}}^{(2)}(e_2^{(1)}), \tag{18}$$

where j = 1, 2, ..., n. The terms $\frac{-\partial E}{\partial m_{1j}^{(2)}}$ and $\frac{-\partial E}{\partial m_{2j}^{(2)}}$ are calculated in the following

$$\begin{aligned}\frac{-\partial E}{\partial m_{1j}^{(2)}}&=\delta_{1j}^{(2)}\cdot\frac{\partial \mu_{\tilde{F}_{1j}}^{(2)}(e_2^{(1)})}{\partial m_{1j}^{(2)}}\\&=\delta_{1j}^{(2)}\cdot\exp\left\{-\frac{1}{2}\left(\frac{e_2^{(1)}-m_{1j}^{(2)}}{\sigma_{1j}^{(2)}}\right)^2\right\}\cdot\frac{(e_2^{(1)}-m_{1j}^{(2)})}{(\sigma_{1j}^{(2)})^2},\end{aligned} \tag{19}$$

$$\begin{aligned}\frac{-\partial E}{\partial m_{2j}^{(2)}}&=\delta_{2j}^{(2)}\cdot\frac{\partial \mu_{\tilde{F}_{2j}}^{(2)}(\dot{e}_2^{(1)})}{\partial m_{2j}^{(2)}}\\&=\delta_{2j}^{(2)}\cdot\exp\left\{-\frac{1}{2}\left(\frac{\dot{e}_2^{(1)}-m_{2j}^{(2)}}{\sigma_{2j}^{(2)}}\right)^2\right\}\cdot\frac{(\dot{e}_2^{(1)}-m_{2j}^{(2)})}{(\sigma_{2j}^{(2)})^2},\end{aligned} \tag{20}$$

in which j = 1, 2, ..., n. Similarly, the computations of $\frac{-\partial E}{\partial \sigma_{1j}^{(2)}}$ and $\frac{-\partial E}{\partial \sigma_{2j}^{(2)}}$ are explained as follows

$$\begin{aligned}\frac{-\partial E}{\partial \sigma_{1j}^{(2)}}&=\delta_{1j}^{(2)}\cdot\frac{\partial \mu_{\tilde{F}_{1j}}^{(2)}(e_2^{(1)})}{\partial \sigma_{1j}^{(2)}}\\&=\delta_{1j}^{(2)}\cdot\exp\left\{-\frac{1}{2}\left(\frac{e_2^{(1)}-m_{1j}^{(2)}}{\sigma_{1j}^{(2)}}\right)^2\right\}\cdot\frac{(e_2^{(1)}-m_{1j}^{(2)})^2}{(\sigma_{1j}^{(2)})^3},\end{aligned} \tag{21}$$

$$\frac{-\partial E}{\partial \sigma_{2j}^{(2)}} = \delta_{2j}^{(2)} \cdot \frac{\partial \mu_{\tilde{F}_{2j}}^{(2)}(\dot{e}_2^{(1)})}{\partial \sigma_{2j}^{(2)}}$$
$$= \delta_{2j}^{(2)} \cdot \exp\left\{-\frac{1}{2}\left(\frac{\dot{e}_2^{(1)} - m_{2j}^{(2)}}{\sigma_{2j}^{(2)}}\right)^2\right\} \cdot \frac{(\dot{e}_2^{(1)} - m_{2j}^{(2)})^2}{(\sigma_{2j}^{(2)})^3}, \quad (22)$$

where j = 1, 2, ..., n.

V. SIMULATION AND EXPERIMENTAL RESULTS

The physical parameters of the ball and beam system are listed in Table 1. The parameters for the FLC and FNN controllers need to be determined a priori.

1) Outer-loop FLC controller:

The rule table for FLC is listed in Table 2. To explain the idea of rule design, the following discussion is helpful. Consider that e1 is PB and $\dot{e}_1$ is PB. In this case, the ball is close to and moves toward to the pivot. To make the ball balanced at the center, a clockwise rotation is required for the beam control, i.e. x2d is NB. Similarly, if e1 is NB and $\dot{e}_1$ is NB, the ball is far away and moves away from the pivot. Again, to move the ball toward the center, the beam has to rotate in a counterclockwise direction, i.e. x2d is PB. In this paper, the means, standard deviations and weighting of the membership functions are given as

$[m_{i1}, m_{i2}, m_{i3}, m_{i4}, m_{i5}] = [-1,-0.5,0,0.5,1]$,

$[\sigma_{i1}, \sigma_{i2}, \sigma_{i3}\sigma_{i4}, \sigma_{i5}] = [0.19,0.19,0.19,0.19,0.19]$,

$[w_1, w_2, w_3, w_4, w_5] = [-1,-0.5,0,0.5,1]$, i = 1, 2,

The scaling factors of the outer-loop is initially set as ISF1=5, ISF2=1 and OSF1=0.5. The input and output membership functions of the outer loop FLC are shown as Fig. 4.

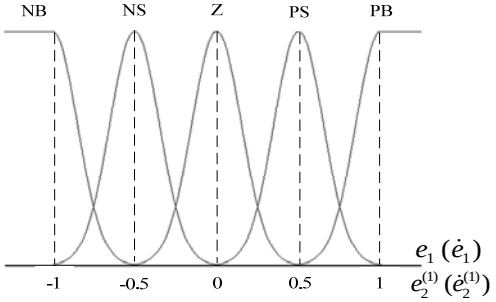

(a)

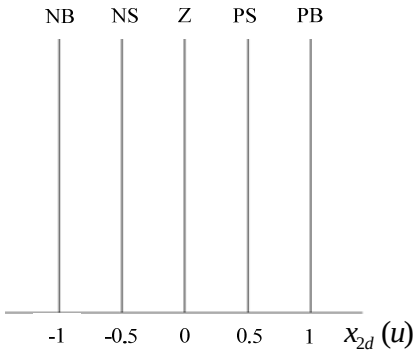

(b)

Fig. 4. Membership functions of the outer-loop FLC and inner-loop FNN: (a) input membership functions, (b) output membership functions.

Table 2. Rule table of FLC

e_1 / $\dot{e}_1$	PB	PS	Z	NS	NB
PB	NB	NB	NB	NS	Z
PS	NB	NB	NS	Z	PS
Z	NB	NS	Z	PS	PB
NS	NS	Z	PS	PB	PB
NB	Z	PS	PB	PB	PB

2) Inner-loop FNN controller:

The parameters of FNN are given in Table 3. The associate scaling factors and learning rates are initially chosen as ISF3=2, ISF4=1, OSF2=12, η_m = 0.1, η_σ = 0.1 and η_w= 0.1. The rule table of FNN is listed in Table 4. To explain the design ideas, the case that $e_2^{(1)}$ is PB and $\dot{e}_2^{(1)}$ is PB is considered. Under this circumstance, x_{2d} is much larger than x_3, and $\dot{x}_{2d}$ is much larger than $\dot{x}_3$. To make the beam angle x_3 track to x_{2d}, the motor has to provide positive high voltage to make the beam rotate fast in a counterclockwise direction, i.e. u is PB. Similarly, if $e_2^{(1)}$ is NB and $\dot{e}_2^{(1)}$ is NB, a negative high voltage from the motor is required such that the beam can rotate fast in a clockwise direction. The input and output membership functions of the FNN are shown in Fig. 4. From (4)-(22), the procedure about the FNN parameter updating is summarized in Fig. 5., where N denotes the maximum iteration number.

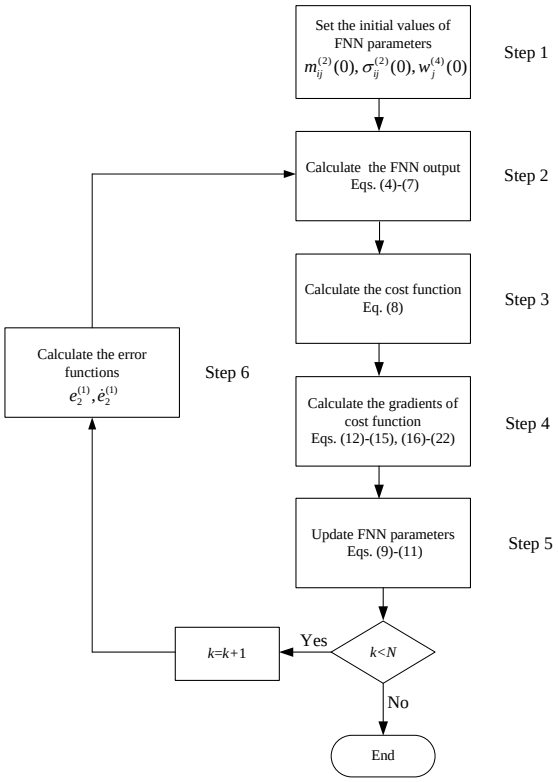

Fig. 5. The procedure of parameter-learning of FNN.

Table 3. Parameters of FNN

j	1	2	3	4	5	6	7	8	9
$\sigma_{ij}^{(2)}$	.15	.15	.15	.15	.15	.15	.15	.15	.15
$m_{1j}^{(2)}$	-1	-1	-1	-1	-1	-.5	-.5	-.5	-.5
$m_{2j}^{(2)}$	-1	-.5	0	.5	1	-1	-.5	0	.5
$w_j^{(4)}$	-1	-1	-1	-.5	0	-1	-1	-.5	0
j	10	11	12	13	14	15	16	17	18
$\sigma_{ij}^{(2)}$	.15	.15	.15	.15	.15	.15	.15	.15	.15
$m_{1j}^{(2)}$	-.5	0	0	0	0	0	.5	.5	.5
$m_{2j}^{(2)}$	1	-1	-.5	0	.5	1	-1	-.5	0
$w_j^{(4)}$	.5	-1	-.5	0	.5	1	-.5	0	.5
j	19	20	21	22	23	24	25		
$\sigma_{ij}^{(2)}$	.15	.15	.15	.15	.15	.15	.15		
$m_{1j}^{(2)}$	.5	.5	1	1	1	1	1		
$m_{2j}^{(2)}$	.5	1	-1	-.5	0	.5	1		
$w_j^{(4)}$	1	1	0	.5	1	1	1		

Table 4. Rule table of FNN

$\dot{e}_2^{(1)}$ \ $e_2^{(1)}$	PB	PS	Z	NS	NB
PB	PB	PB	PB	PS	Z
PS	PB	PB	PS	Z	NS
Z	PB	PS	Z	NS	NB
NS	PS	Z	NS	NB	NB
NB	Z	NS	NB	NB	NB

As shown in Fig. 2, a cascaded FLC-FNN control scheme is proposed for a ball and beam system. In Fig. 2, a FLC is adopted in the outer loop control, and a FNN is considered for the inner loop control. To validate the control performance, an energy-based balance control (EBBC) [6] and the cascade FLC-FLC [7] are also considered. In all simulations, the initial conditions of state variables are $x_1(0)$ = 0.38m, $x_2(0) = x_3(0) = x_4(0) = 0$. The control goal is to stably balance the ball at the position x_{1d} = 0.2m.

The simulation results of the nominal case are shown in Figs. 6-11, including the responses of ball, beam, control signal and the parameter learning of FNN. From Fig. 6, it can be seen that there exists somewhat steady-state error of the ball position using the FLC-FLC and EBBC. In addition, the proposed FLC-FNN has a faster convergence rate of ball balancing. In Figs. 9-11, the parameters of FNN can be asymptotically convergent to some constants.

In addition, the simulation results subject to perturbations are shown in Figs. 12-17. To investigate the control robustness, a uniformly distributed random noise is added to the inner loop continuously, where the feedback signal is x_3+0.02rand(·), rand(·)∈[-1,1]. Furthermore, an external disturbance is considered, where an exogenous torque to the ball is added at the instant of 15sec. In Fig. 12, simulation results indicate that the deviations of the ball position become more significant using the EBBC and FLC-FLC. It can be also seen that the ball moves away from its balance position after the disturbance is added. From Fig. 13, the beam has to rotate counterclockwisely to make the ball move back to x_1=0.2m. It reveals that the proposed FLC-FNN method can effectively achieve the goal of ball balance and the problems of uncertainties can be also deal with. The parameters of FNN are shown in Figs. 15-17, where all updating parameters can asymptotically converge to some constants.

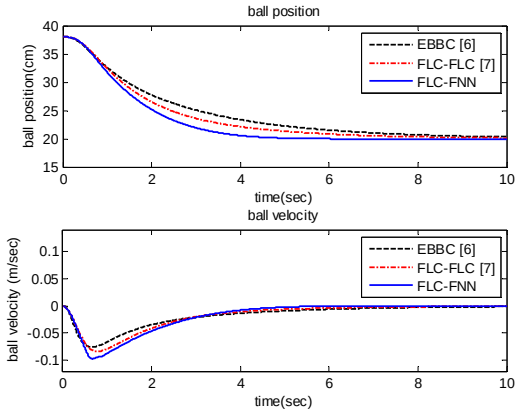

Fig. 6. Responses of the ball: position (top) and velocity (bottom).

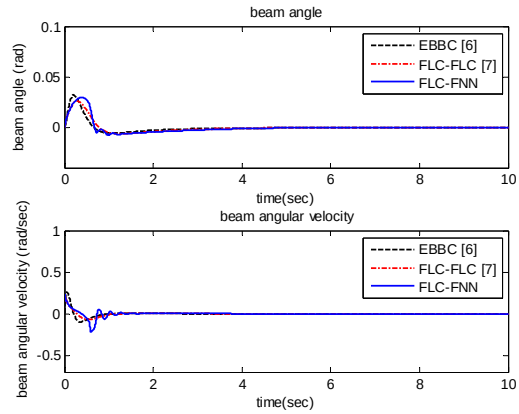

Fig. 7. Responses of the beam: angle (top) and angular velocity (bottom).

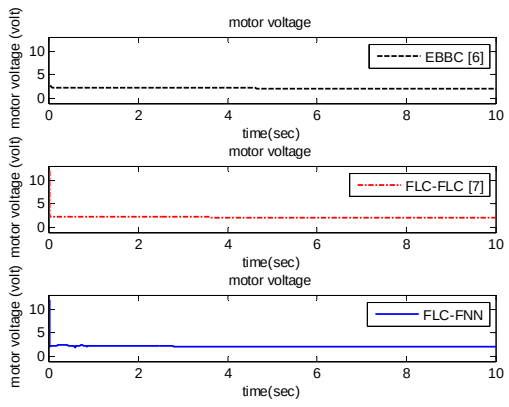

Fig. 8. Responses of control signal.

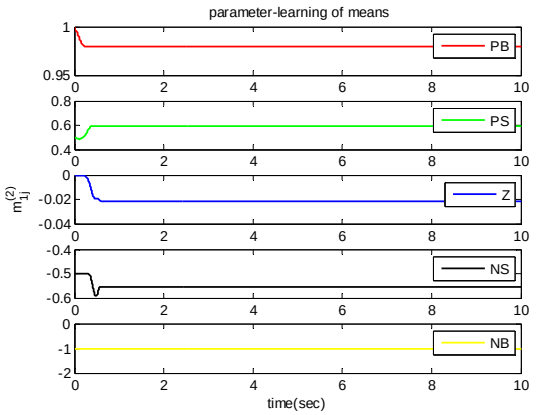

Fig. 9. Parameter-learning of $m_{1j}^{(2)}$.

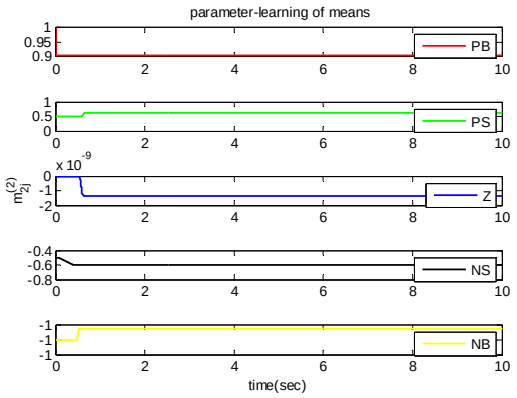

Fig. 10. Parameter-learning of $m_{2j}^{(2)}$.

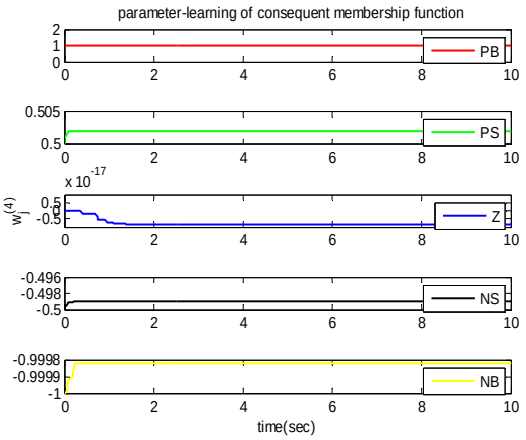

Fig. 11. Parameter-learning of $w_j^{(4)}$.

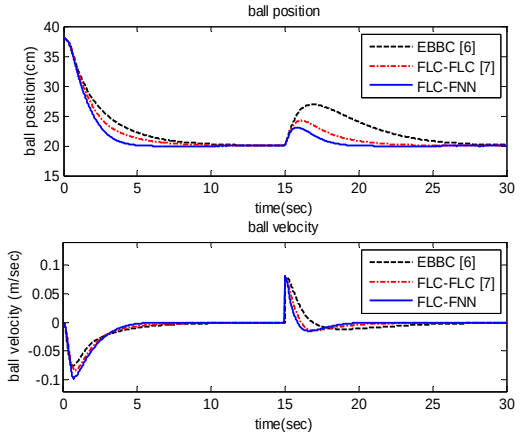

Fig. 12. Responses of the ball: position (top) and velocity (bottom).

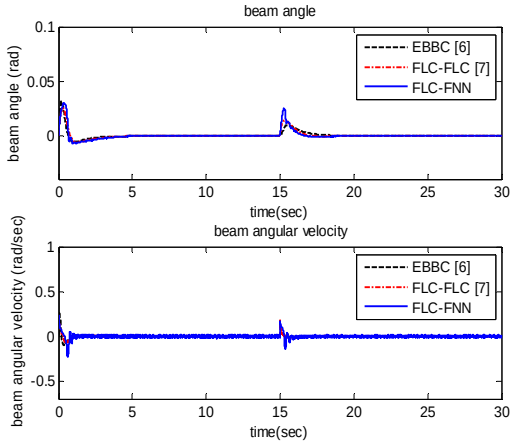

Fig. 13. Responses of the beam: angle (top) and angular velocity (bottom).

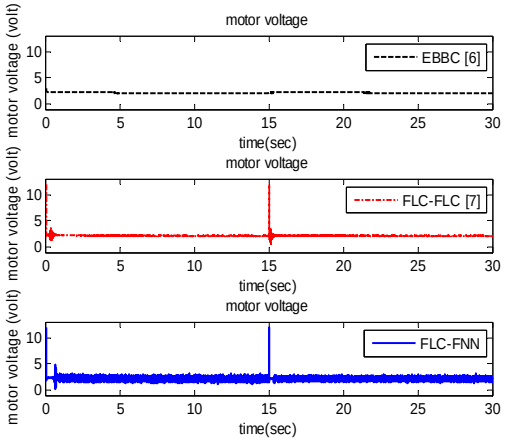

Fig. 14. Responses of control signals.

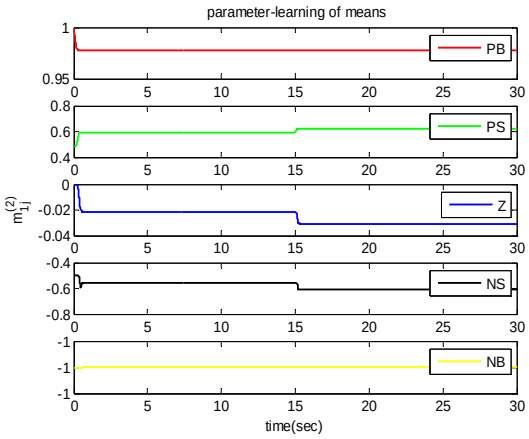

Fig. 15. Parameter-learning of $m_{1j}^{(2)}$.

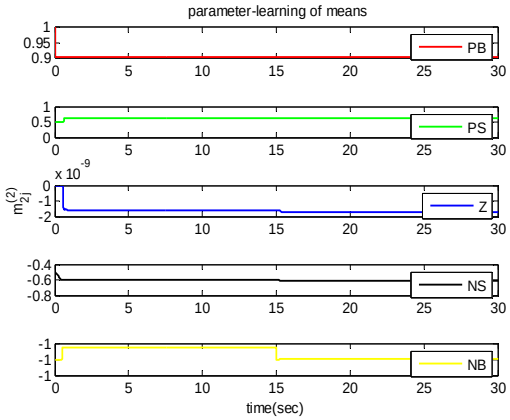

Fig. 16. Parameter-learning of $m_{2j}^{(2)}$.

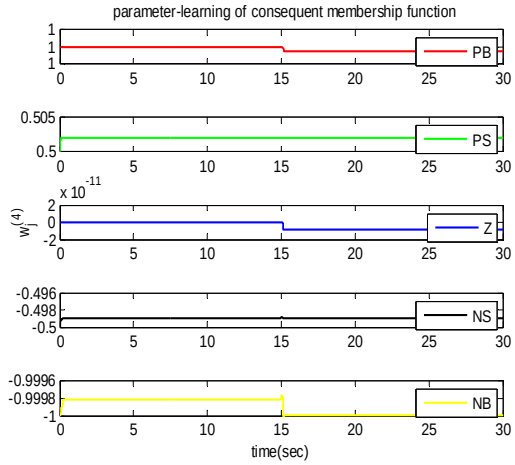

Fig. 17. Parameter-learning of $w_j^{(4)}$.

The experimental setup of a ball and beam control system is shown in Fig. 18, where the system consists of a mechanical frame, a DC motor, a position sensor, an actuator, an A/D converter, and a digital control platform. The control scheme of the ball and beam system is shown in Fig. 19, including a DSP (TMS320C6713) and a FPGA (FlexEPF10k70) development boards. The FPGA is the interface between the DSP and external signals. The main tasks of the FPGA are signal processing and external devices controlling, such as the A/D converter, the pulse width modulation (PWM) generator, the motor speed encoder and the DSP/FPGA interface. The proposed control kernel is embedded in the DSP chip. The sampling period of all experiments is selected to be 1ms.

In all experiments, the initial conditions of state variables are the same as that given in simulations, $\mathbf{x}(0) = [0.38\ 0\ 0\ 0]^T$. The measured responses corresponding to the nominal case are shown in Figs. 20-22, including the responses of ball, beam, and control signal. From Fig. 20, it can be seen that there exists significant steady-state error of the ball position using the EBBC. Moreover, it can be observed that the FLC-FNN controller can provide smoother and faster trajectories than that of FLC-FLC.

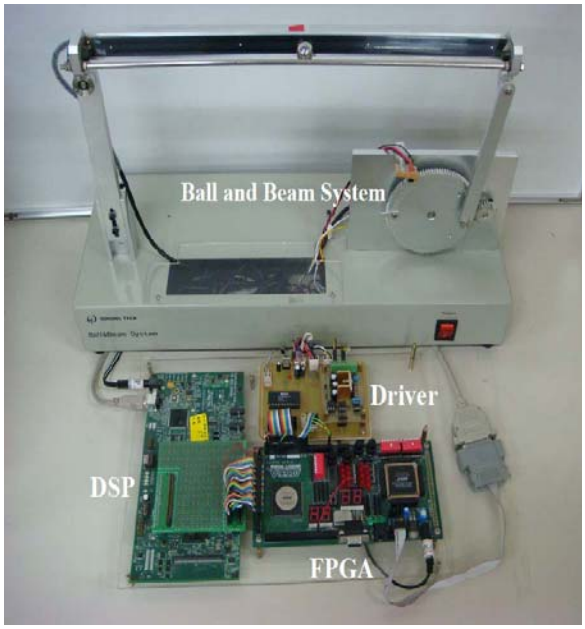

Fig. 18. Experiment setup of the ball and beam system.

The experiment results of perturbation cases are shown in Figs. 23-25. In the perturbation cases, an artificial external disturbance is added in the time interval 10 sec to 10.3 sec, such that x_1 becomes x_1+0.05m. The added deviation can be considered as the measurement noise of ball position. From Fig. 23, it can be seen that the proposed FLC-FNN provides better responses than the counterparts of EBBC and FLC-FLC in the aspect of tracking accuracy and robustness. From Figs. 6 and 20, the experimental response has larger overshoot and time-delay compared with the simulation results. That is because the friction effects of gears and beam are ignored in simulations.

VI. CONCLUSIONS

In this paper, a FLC-FNN control scheme is proposed for a ball and beam system, in which noise and disturbance are considered. The network structure and theoretical bases of the proposed FNN control system are described in detail. The update laws of FNN parameters are obtained based on the gradient decent method. In the design of the FLC-FNN, no constrained conditions and prior knowledge of the controlled plant are required. Finally, simulation and experimental results illustrate that the proposed FLC-FNN can provide better performances than FLC-FLC and EBBC counterparts.

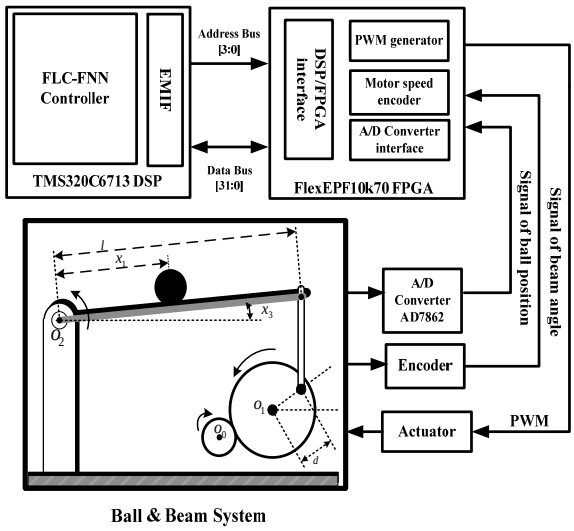

Fig. 19. Control scheme of the ball and beam system.

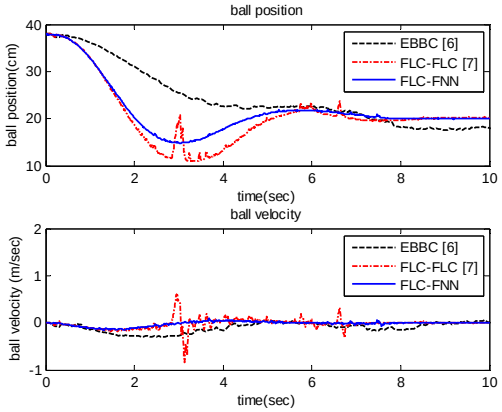

Fig. 20. Responses of the ball: position (top) and velocity (bottom).

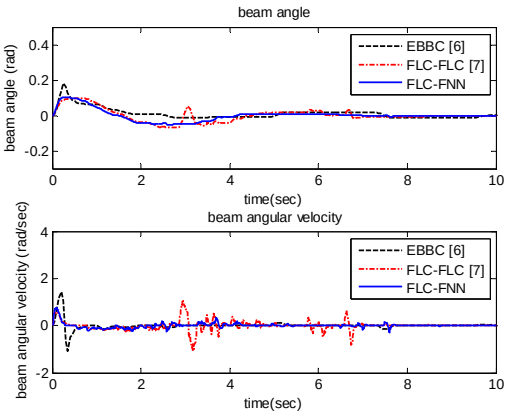

Fig. 21. Responses of the beam: angle (top) and angular velocity (bottom).

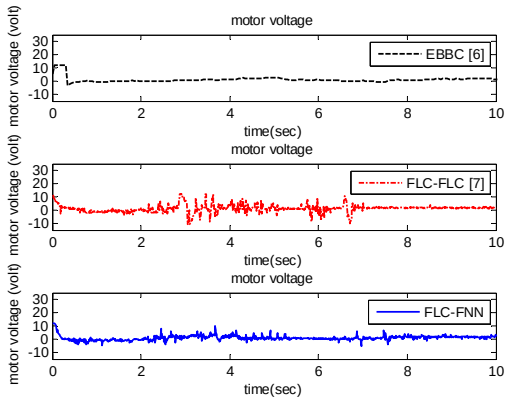

Fig. 22. Responses of control signal.

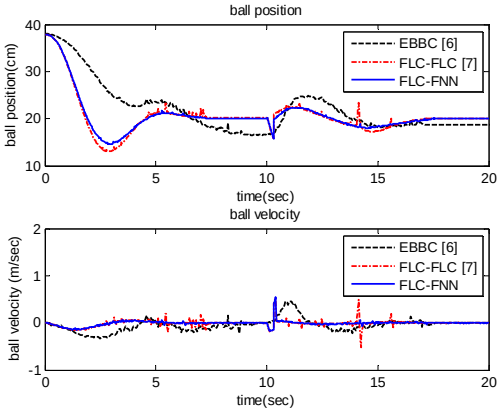

Fig. 23. Responses of the ball: position (top) and velocity (bottom).

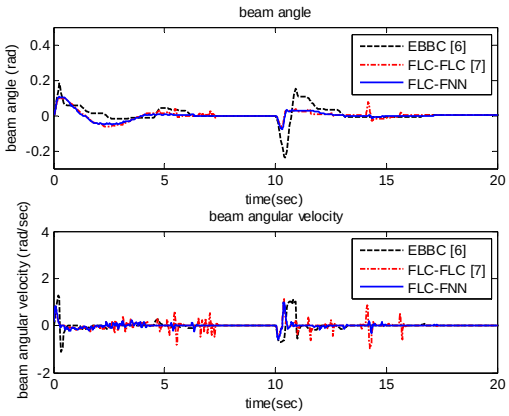

Fig. 24. Responses of the beam: angle (top) and angular velocity (bottom).

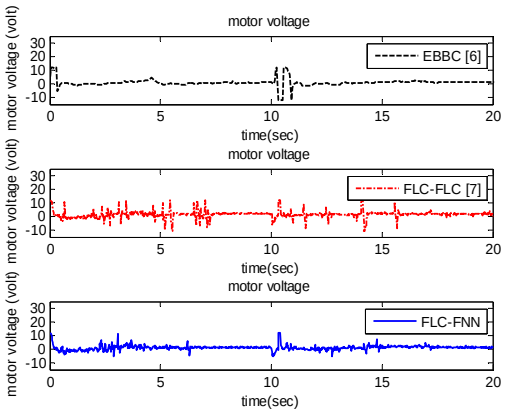

Fig. 25. Responses of control signal.

REFERENCES

[1] Hua, M. D., Hamel, T., Morin, P., and Samson, C., "A control approach for thrust-propelled underactuated vehicles and its application to VTOL Drones," *IEEE Trans. on Automatic Control*, Vol. 54, No. 8, pp.1837-1853, 2009.

[2] Sankaranarayanan, V. and Mahindrakar, A. D., "Control of a class of underactuated mechanical systems using sliding modes," *IEEE Trans. on Robotics*, Vol. 25, No. 2, pp.459-467, 2009.

[3] Børhaug, E., Pavlov, A., Panteley, E., and Pettersen, K. Y., "Straight line path following for formations of underactuated marine surface vessels," *IEEE Trans. on Control Systems Technology*, Vol. 19, No. 3, pp. 493-506, 2011.

[4] Cabecinhas, D., Naldi, R., Marconi, L., Silvestre, C., and Cunha, R., "Robust take-off for a quadrotor vehicle," *IEEE Trans. on Robotics*, Vol. 28, No. 3, pp.734-742, 2012.

[5] Nodland, D., Zargarzadeh, H., and Jagannathan, S. "Neural network-based optimal adaptive output feedback control of a helicopter UAV," *IEEE Trans. on Neural Networks and Learning Systems*, Vol. 24, No. 7, pp.1061-1073, 2013.

[6] Li, E., Liang, Z.-Z., Hou, Z.-G., and Tan, M., "Energy-based balance control approach to the ball and beam system," *International Journal of Control*, Vol. 82, No. 6, pp. 981-992, 2009.

[7] Oh, S. K., Jang, H. J., and Pedrycz, W., "The design of a fuzzy cascade controller for ball and beam system: a study in optimization with the use of parallel genetic algorithms," *Engineering Applications of Artificial Intelligence*, Vol. 22, No.2, pp. 261-271, 2009.

[8] Khuntia, S. R., Mohanty, K. B., Panda, S., and Ardil, C., "A comparative study of P-I, I-P, fuzzy and neuro-fuzzy controllers for speed control of dc motor drive," *International Journal of Electrical and Computer Engineering*, Vol. 5, No. 5, pp. 287-291, 2010.

[9] Chang, P. H. and Jung, J. H., "A systematic method for gain selection of robust PID control for nonlinear plants of second-order controller canonical form," *IEEE Trans. on Control Systems Technology*, Vol. 17, No. 2, pp. 473-483, 2009.

[10] Lee, C. C., "Fuzzy logic in control systems: fuzzy logic controller-part I," *IEEE Trans. on Systems, Man and Cybernetics*, Vol. 20, No. 2, pp. 404-418, 1990.

[11] Pedrycz, W., *Fuzzy Control and Fuzzy Systems*, NY: Wiley, 1993.

[12] Tao, C. W. and Taur, J. S., "Robust fuzzy control for a plant with fuzzy linear model," *IEEE Trans. on Fuzzy Systems*, Vol. 13, No. 1, pp. 30-41, 2005.

[13] Chiu, C. S., "Mixed feedforward/feedback based adaptive fuzzy control for a class of MIMO nonlinear Systems," *IEEE Trans. on Fuzzy Systems*, Vol. 14, No. 6, pp. 716-727, 2006.

[14] Chang, Y.-H., Chang, C.-W., Taur, J. S., and Tao, C. W., "Fuzzy swing-up and fuzzy sliding-mode balance control for a planetary-gear-type inverted pendulum," *IEEE Trans. on Industrial Electronics*, Vol. 56, No. 9, pp. 3751-3761, 2009.

[15] Khedri, J., Chaabane, M., Souissi, M., and Mehdi, D., "Speed control of a permanent magnet synchronous machine (PMSM) fed by an inverter voltage fuzzy control approach," *International Journal of Electrical and Computer Engineering*, Vol. 5, No. 6, pp. 342-348, 2010.

[16] Lin, F.-J. and Shen, P.-H., "Adaptive fuzzy-neural-network control for a DSP-based permanent magnet linear synchronous motor servo drive," *IEEE Trans. on Fuzzy Systems*, Vol. 14, No. 4, pp. 481-495, 2006.

[17] Wai, R.-J. and Lee, J.-D. "Robust levitation control for linear maglev rail system using fuzzy neural network," *IEEE Trans. on Control Systems Technology*, Vol. 17, No. 1, pp. 4-14, 2009.

[18] Yuan, X., Wang, Y., Wu, L., Zhang, X., and Sun, W., "Neural network based self-learning control strategy for electronic throttle valve," *IEEE Trans. on Control Systems Technology*, Vol. 59, No. 8, pp. 3757-3765, 2010.

[19] Singh, M. and Chandra, A., "Application of adaptive network-based fuzzy inference system for sensorless control of

PMSG-based wind turbine with nonlinear-load-compensation capabilities," *IEEE Trans. on Power Electronics*, Vol. 26, No. 1, pp. 165-175, 2011.

[20] Chang, Y.-H., Chan, W.-S., Chang, C.-W., Hsu, C.-H., and Tao, C.W., "Adaptive fuzzy control for under-actuated ball and beam system with virtual state following," *The 9th WSEAS Int. Conf. on Robotics, Control and Manufacturing Technology*, pp. 136-141, 2009.

[21] Chang, Y.-H., Chan, W.-S., and Chang, C.-W., "T-S fuzzy model based adaptive dynamic surface control for ball-and-beam system," *IEEE Trans. Ind. Electron.*, Vol. 60, No. 6, pp. 2251-2263, 2013.

[22] Lin, F.-J., Wai, R.-J., and Lee, C.-C., "Fuzzy neural network position controller for ultrasonic motor drive using push-pull DC-DC converter," *IEE Proceedings: Control Theory and Applications*, Vol. 146, No. 1, pp. 99-107, 1999.